ORGANIC CHEMISTRY FRONTIERS

RESEARCH ARTICLE

View Article Online
View Journal | View Issue

Cite this: *Org. Chem. Front.*, 2021, **8**, 3659

Dual-stimuli pseudorotaxane switches under kinetic control†‡

Marius Gaedke, [a] Henrik Hupatz,[a] Hendrik V. Schröder, §[a] Simon Suhr,[b] Kurt F. Hoffmann, [c] Arto Valkonen, [d] Biprajit Sarkar, [b] Sebastian Riedel, [c] Kari Rissanen [d] and Christoph A. Schalley *[a]

A series of dumbbell-shaped *sec*-ammonium salts with bulky (pseudo)stoppers ('speed bumps') were tested for their ability to form pseudorotaxanes with a redox-switchable, tetrathiafulvalene (TTF)-decorated [24]crown-8 ether. Depending on the size of the pseudostoppers, fast (less than ten minutes), slow (hours to days) and very slow (no pseudorotaxanes observed) threading has been observed. NMR spectroscopy as well as tandem mass spectrometry indicate the formation of non-threaded face-to-face complexes prior to pseudorotaxanes formation. Both isomers can be distinguished by their substantially different stability in collision-induced dissociation (CID) experiments. Two external stimuli affect the stability of the pseudorotaxanes: Deprotonation of the ammonium ion results in fast dethreading, while dethreading is much slower when induced by the charge repulsion upon chemical oxidation of the TTF moiety. Remarkably, the same steric bulk of the pseudostopper thus leads to different dethreading rates depending on the stimulus applied. Based on these findings, two redox-switchable rotaxanes containing a 1-naphthyl and a phenyl moiety as sterically different 'speed bumps' in the axle centre were synthesised. Bulk electrolysis of the rotaxanes did not result in the expected macrocycle translocation on the axle independent of the 'speed bump' as a remarkable consequence of the mechanical bond.

Received 31st March 2021,
Accepted 28th April 2021

DOI: 10.1039/d1qo00503k

rsc.li/frontiers-organic

Introduction

Artificial molecular switches[1] are controlled by external chemical,[2,3] light,[4,5] or electrochemical[6] stimuli. In mechanically interlocked molecules (MIMs) such as rotaxanes and catenanes, stimuli-induced switching manipulates the interactions of the wheels with their binding sites on the other component in a controlled manner.[7,8] Pseudorotaxanes are non-interlocked, but threaded axle-wheel complexes able to dissociate without breaking a covalent bond. Depending on the bulkiness of the axle end groups, they encompass a broad range of dethreading rates with the rotaxane at the very end, where no wheel exchange takes place (Fig. 1a).[9] Thus, (pseudo)rotaxanes allow us to study stimuli-induced switching with and without wheel exchange. In rotaxanes, the wheel's translational freedom is limited to the track provided by the axle[10] and switching can be converted into directed co-conformational changes, which can propel artificial molecular motors and machines.[7,8,11] The impact of the wheel exchange rate on dual-stimuli-induced switching has not been studied for kinetically hindered pseudorotaxanes, but rather for pseudorotaxanes with fast exchange or for rotaxanes (no exchange). This raises an interesting question: Can different stimuli applied to a dual-stimuli-responsive *and* kinetically hindered pseudorotaxane result in different timescales for dethreading over a 'speed bump' pseudostopper, even when the steric size of the 'speed bump' remains unchanged?

The energy landscapes of switchable (pseudo)[2]rotaxanes change, when stimuli are applied. In Fig. 1, which exemplarily depicts an acid/base- *and* redox-switchable pseudorotaxane (Fig. 1b and c) and its 'speed bump' containing rotaxane analogue (Fig. 1d and e), the yellow dots represent the (pseudo) rotaxane populations. Initially, the wheels reside on the binding site. Upon applying one of the two stimuli, the former binding site becomes disfavoured and the macrocycles migrate over the blue 'speed bump'. For the pseudo[2]rotaxane, the wheel is released from the axle over the barrier caused by the

[a]*Institut für Chemie und Biochemie der Freien Universität Berlin, Arnimallee 20, 14195 Berlin, Germany. E-mail: c.schalley@fu-berlin.de*
[b]*Lehrstuhl für Anorganische Koordinationschemie, Institut für Anorganische Chemie, Universität Stuttgart, Pfaffenwaldring 55, 70569 Stuttgart, Germany*
[c]*Institut für Chemie und Biochemie der Freien Universität Berlin, Fabeckstr. 34/36 14195, Berlin, Germany*
[d]*Department of Chemistry P.O. Box 35, 40014 Jyväskylä, Finland*

† Dedicated to Prof. Placido Neri upon the occasion of his 60th birthday.

‡ Electronic supplementary information (ESI) available. CCDC 2073308. For ESI and crystallographic data in CIF or other electronic format see DOI: 10.1039/d1qo00503k

§ Present address: Dr H. V. Schröder Department of Chemical and Biological Engineering, Princeton University, Princeton, NJ08544, USA

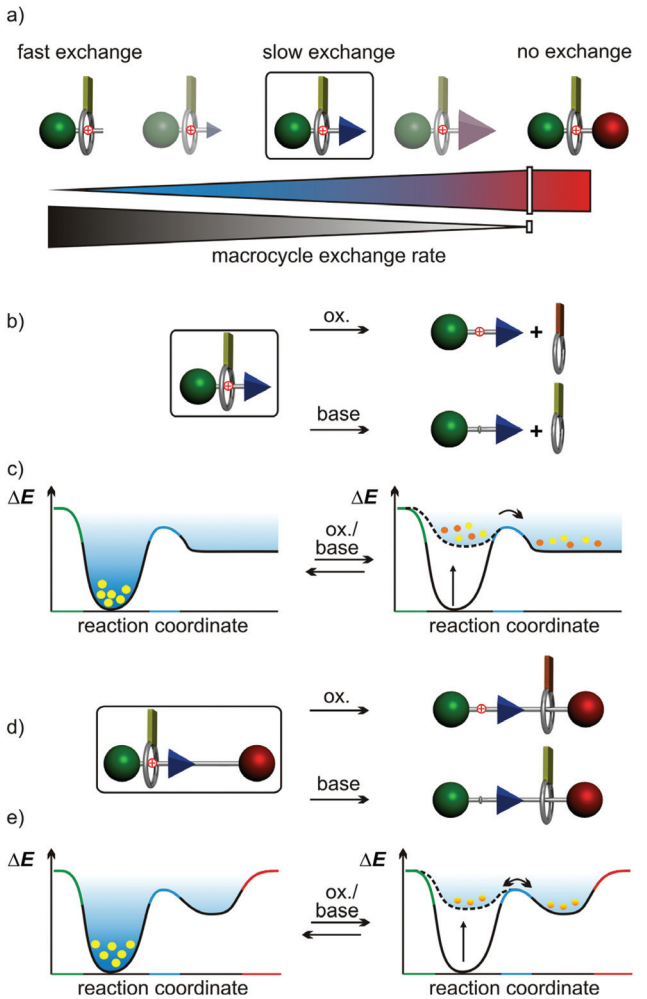

Fig. 1 (a) Range of macrocycle exchange rates from a quickly reversible pseudorotaxane formation (light blue, small 'speed bump') to a fully interlocked rotaxane (red stopper). (b) Stimuli-induced shuttling or unthreading and (c) the corresponding changes of the energy landscapes of a pseudorotaxane as well as (d and e) of a rotaxane (stoppers: green/red, steric 'speed bump' in the axle: blue, TTF oxidation states in yellow (reduced)/orange (oxidized to TTF^{2+}).

pseudostopper, while the wheel cannot escape from the axle in the [2]rotaxane. It will nevertheless move across the 'speed bump' back and forth and a new equilibrium distribution of positional isomers is finally reached on a time scale depending on the 'speed bump' size.

From the broad variety of available binding motifs,[12,13] *sec*-ammonium/crown ether (pseudo)rotaxanes provide an easy access to dual-stimuli-responsive compounds that allow us to investigate the above question in detail. In this motif, a crown ether encircles the ammonium ion with binding constants typically in the range of 10^2 to 10^6 M^{-1} in non-protic organic solvents. In thermodynamic terms, ammonium ions form threaded complexes depending on the number of hydrogen bonds (including C–H···O hydrogen bonds involving the methylene groups next to the ammonium ion), charge distribution and ion pair separation energies of the ammonium

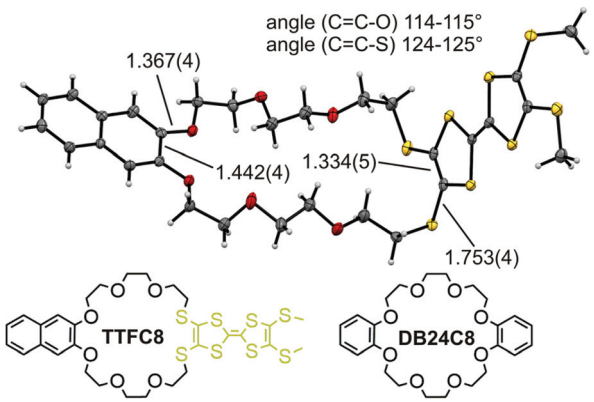

Fig. 2 Solid-state structure of **TTFC8** with selected bond lengths (Å) and angles.

salt.[14,15] Only face-to-face interactions are possible,[16] when the axle end groups are sterically too bulky. A large number of pseudo[2]rotaxanes with different crown ether sizes and different end groups have been reported to form in a broad variety of solvents.[17–19] In marked contrast, only few examples of rotaxanes with 'speed bumps' along their axles have been studied to unravel the influence of the mechanical bond.[20–25] The studies on shuttling in crown ether rotaxanes mostly focus on degenerate shuttles with two or more equivalent binding sites.[20,24] However, non-degenerate shuttles are more suitable for directional movement,[26] among which only very few are responsive to both acid/base and redox stimuli.[27]

Here, we make use of the *sec*-ammonium/crown ether binding motif and describe a series of pseudorotaxanes responsive to both stimuli with differently sized and differently shaped pseudostoppers. The ammonium/crown ether interaction can be disrupted by deprotonation of the ammonium group with a strong base.[28] Introducing a tetrathiafulvalene (TTF) into the crown ether (**TTFC8**, Fig. 2) implements also the second stimulus: Two-electron oxidation of the TTF unit to its dication induces coulombic repulsion between the wheel and the ammonium station and is expected to lead to dethreading as well.[29,30] Hence, these dual-stimuli-responsive pseudorotaxanes allow comparing the dethreading rates after deprotonation with those after oxidation, while maintaining the same steric bulk of the 'speed bump' pseudostopper. After identifying a suitable pseudostopper in pseudorotaxane dethreading experiments, this 'speed bump' can be integrated into a rotaxane axle to investigate co-conformational changes in the dual-stimuli-responsive [2]rotaxane, in which the mechanical bond prevents dethreading.

Results and discussion

The wheel: crystal structure of TTFC8

The redox-active wheel **TTFC8** used in this study was synthesized as reported earlier.[29] This macrocycle and the commercially available and widely used dibenzo[24]crown-8 ether (**DB24C8**) have the same number of 24 atoms along their cir-

cumference. Nevertheless, the substitution of two catechol oxygen by sulfur atoms affects both the structure and the conformational properties of the ring,[31] as becomes clear, when comparing the new solid state structure of **TTFC8** (Fig. 2, also see ESI section 8‡) with the known structure of **DB24C8**.[31]

The naphthalene-substituted side of **TTFC8** only shows a minor elongation in the central C=C bond (1.44 Å compared to 1.41 Å for **DB24C8**), the C–O bond lengths and C=C–O angles are virtually the same (1.37 Å and 115°). Although a shorter central C=C bond (1.33 Å) can be found on the TTF side, the C–S bond lengths (1.75 Å *vs.* 1.37 Å) and C=C–S bond angles (125° *vs.* 115°) notably enlarge the macrocycle cavity on the TTF-substituted side consistent with other published thiacrown derivatives.[32–34] The S atoms are *exo* to the ring rather than *endo*, like the oxygens on the other side. The effect of the structure on binding ammonium guests was investigated in our previous paper.[30]

Threading experiments

To test whether these differences in ring annulus lower the barrier to overcome bulky substituents, various *sec*-ammonium axles were synthesised as tetrakis(3,5-bis(trifluoromethyl) phenyl) borate ($BArF_{24}^-$) salts to compensate for the reduced binding constants of the thiacrown (see ESI section 5‡ for details).[29] Using $BArF_{24}^-$ with respect to PF_6^- results in a 10 to 20-fold increase of the binding constant.[30] The axles only differ in their terminal groups on one side (shown in blue in Fig. 3). As a guideline for the pseudostopper size and shape literature data available for **DB24C8**-based (pseudo–)rotaxanes with PF_6^- counterions was used.[16,19,35]

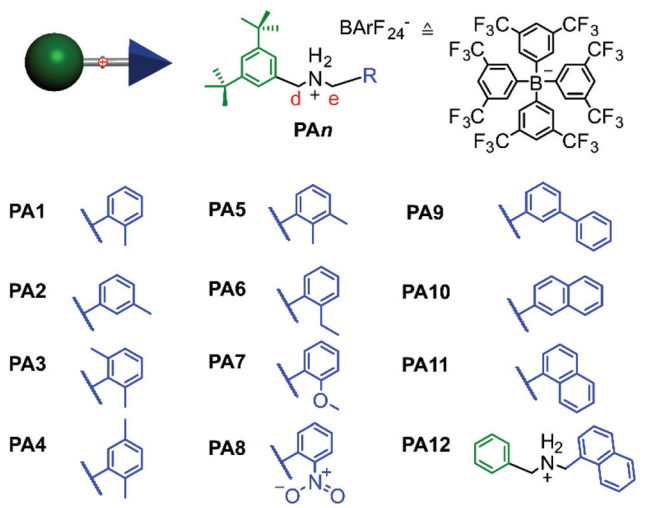

Fig. 3 The synthesised axles PA*n*.

The axles were mixed with either **DB24C8** or **TTFC8** in a 1 : 1 ratio in CD_2Cl_2. ^{1}H NMR spectra were taken at regular intervals to compare the half-lives ($t_{1/2}$) of the threading reactions for 4 mM solutions at room temperature by following the changing integrals of the $C\underline{H}_2$–NH_2–$C\underline{H}_2$ signals (see Table 1 and ESI section 2 Fig. S27–41‡ for the NMR spectra). Upon threading, the two methylene group signals shift downfield ($\Delta\delta \geq +0.2$ ppm). Furthermore, diastereotopic splitting of the crown ether methylene groups is observed for the pseudorotaxanes due to the directionality of the axle.[16,36]

An initial kinetic screening categorizes the axles into three groups. The first group (**PA1**, **PA2**, **PA4**, **PA8**, **PA9** and **PA10**) shows complete conversion into the threaded complex with **TTFC8** and **DB24C8** within less than 10 min. The second group (**PA5**, **PA6**, **PA7** and **PA11**) reveals half-lives in the range of hours to days. In addition, **PA5**, **PA6** and **PA7** form pseudorotaxanes with **TTFC8**, but not with **DB24C8** (even within 14 days). Both crown ethers can, however, pass the 1-naphthalene pseudostopper of **PA11** to form threaded complexes. Here, the slightly larger **TTFC8** threaded onto the axle approximately 120 times more quickly. Finally, no sign of threading is observed for **PA3** neither with **DB24C8** nor **TTFC8** within 14 days. These results are in good agreement with a recent study by Credi *et al.*[19] which also showed the 3,5-dimethyl phenyl moiety to be an efficient stopper in **DB24C8** containing rotaxanes[37–40] and identified the 2,6-dimethyl phenyl moiety as kinetically inert to threading of **DB24C8**.[19] Consequently, out of these candidates we chose **PA11** (1-naphthyl) as the most suitable pseudostopper for dual-stimuli-induced switching experiments, because threading occurs at time intervals that are conveniently observable by NMR spectroscopy.

In summary, the slight differences in size and shape apparent from the comparison of the crystal structures clearly affect the threading kinetics even though **TTFC8** and **DB24C8** share the same number of atoms in the wheel circumference.

Face-to-face complexes *vs.* pseudorotaxanes

In order to obtain some orienting insight into the thermodynamic binding properties of **PA11**, axle **PA12** has been synthesized, which allows fast threading of **TTFC8** over the phenyl group. The association constant obtained by isothermal titration calorimetry amounts to $K_a = (3.9 \pm 0.7)\ 10^5\ M^{-1}$ (ΔG° =

Table 1 Screening of threading timescales in model pseudo[2]rotaxanes PA*n*@MC and their corresponding half-lives $t_{1/2}$ for **DB24C8** and **TTFC8** threading monitored by ^{1}H NMR (4 mM in $CD_2Cl_2/CDCl_3$ 400/500 MHz at r.t.)

Entry[a]	PA1	PA2	PA3	PA4	PA5	PA6	PA7	PA8	PA9	PA10	PA11
DB24C8	<10 min	<10 min	≫14 days	<10 min	≫14 days	≫14 days	≫14 days	<10 min	<10 min	<10 min	10 days
TTFC8	<10 min	<10 min	≫14 days	<10 min	50 h	14 days	22 h	<10 min	<10 min	<10 min	2 h

[a] Axles denoted with "≫14 days" were considered to be not suitable for this study. It does not necessarily exclude a threaded complex to be achievable over time with suitable temperature and concentration.

(-31.9 ± 0.4) kJ mol^{-1}, ΔH° = (-44.1 ± 1.2) kJ mol^{-1}, $T\Delta S^\circ$ = (-12.2 ± 1.6) kJ mol^{-1}; also, see ESI section 5 and Table S2†). This binding data is very similar to that of the symmetrical dibenzylammonium axle (**DBA**) (K_a = (7.7 ± 1.0) 10^5 M^{-1} (ΔG° = (-33.6 ± 0.3) kJ mol^{-1}, ΔH° = (-39.8 ± 1.0) kJ mol^{-1}, $T\Delta S^\circ$ = (-6.2 ± 1.3) kJ mol^{-1}). We therefore assume the binding data for **PA11** to be in a similar range.

An ITC experiment with **PA11** was also attempted with titration intervals of 20 min to account for the slow threading. Remarkably, very sharp heat signals were observed. The quick heat evolution is not consistent with the slow pseudorotaxane formation as observed in ^{1}H NMR experiments. Obviously, the axle and the crown ether quickly form a non-threaded complex (Fig. 4a),[16] for which an upper limit for K_a of *ca.* 10^4 M^{-1} is estimated (see ESI section 5 and Fig. S53‡). ^{1}H NMR experiments confirm this face-to-face complex formation that is expressed in a minor shift for the methylene protons next to the ammonium moiety. These signals vanish slowly over time with the appearance of pseudorotaxane signals (Fig. S41‡).

Besides the evidence from ITC and NMR experiments, tandem mass spectrometry complements the picture. As one can expect the face-to-face complexes to easily dissociate in the gas phase upon collision-induced dissociation (CID), the dethreading of the pseudorotaxanes should require higher collision energies due to the steric barrier caused by the pseudostopper. Fig. 4b shows the survival yield curves for **PA11@TTFC8** separately prepared and isolated by column chromatography (blue) in comparison to a mixture of **PA11** and **TTFC8** subjected to the collision experiment 5 (red) and 135 minutes (black) after sample preparation. The red curve is indicative of a complex, which fragments at rather low collision voltages ($E_{1/2}$ = 9.8 ± 0.2 V). A small amount of 5% of the complex remains intact and half of it is fragmented at *ca.* 39 V. The blue curve shows only one, more stable complex ($E_{1/2}$ = 39.2 ± 0.4 V). For the sample taken after 135 min roughly 40% of the complex fragment at the lower collision voltage, while 60% fragment at the higher one. Clearly, two differently stable complexes form, *i.e.* the instantly forming face-to-face complex and the pseudorotaxane, which increases in abundance over time. This nicely shows the conversion of the instantly formed, but weaker non-threaded complex (lower equilibrium constant K_1, but higher rate constant k_1) into the pseudorotaxane (higher equilibrium constant K_2, but lower rate constant k_2).

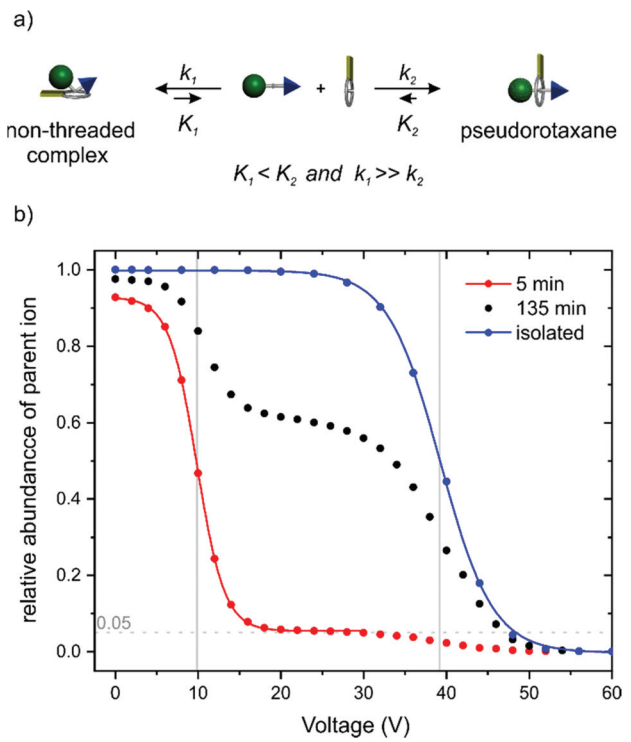

Fig. 4 (a) Schematic representation of the equilibrium for face-to-face complexation which competes with the formation of **PA11@TTFC8**. (b) Survival yield curves obtained for mass-selected [**PA11**·**TTFC8**]$^+$ ions (*m*/*z* 1108) at increasing collision voltages. Red curve: sample 5 min; black curve: sample 135 min after mixing of axle and wheel. Blue curve: pre-formed pseudorotaxane isolated by column chromatography before the experiment. The solid lines represent a sigmoidal fitting to determine 50% survival yield voltages $E_{1/2}$: red: $E_{1/2}$ = (9.8 ± 0.2) V; blue: $E_{1/2}$ = (39.2 ± 0.4) V (for experimental details, see ESI section 3‡).

Dual-stimuli responsiveness

When pseudo[2]rotaxane **PA11@TTFC8** is deprotonated with an excess of polystyrene-immobilized P2 base, quick dethreading is observed (Fig. 5b and ESI section 2 Fig. S32, S34, S36

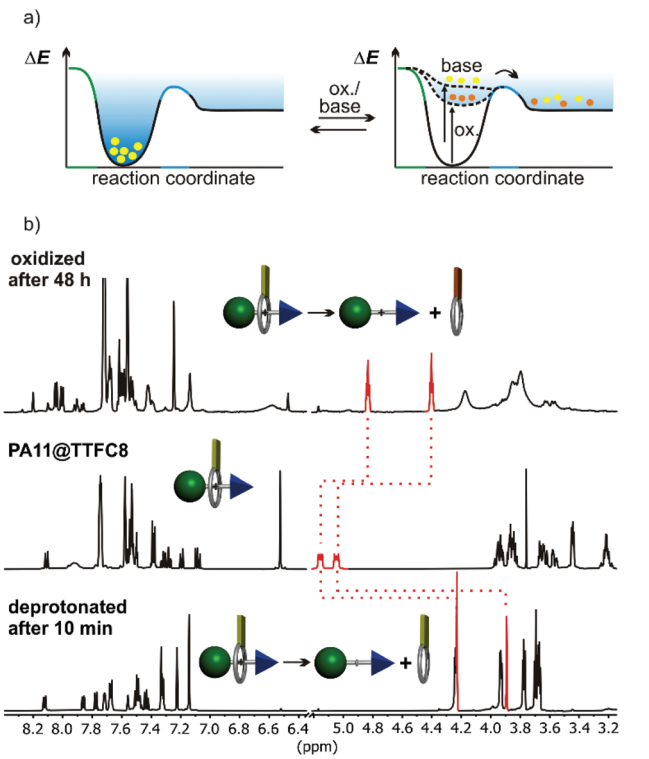

Fig. 5 (a) Dual-stimuli switching expressed in terms of the potential energy surface of the pseudorotaxane **PA11@TTFC8**. (b) ^{1}H NMR spectra (600 MHz, dry CD_2Cl_2, 298 K) of **PA11@TTFC8** (center), 48 hours after oxidation with excess $NOSbF_6$ (top), and 10 minutes after deprotonation with an excess of Schwesinger's P2 base immobilized on polystyrene (bottom).

and S42‡). No indication for hydrogen bonding of neutral **TTFC8** to the neutral axle was observed in the ^{1}H NMR spectra in contrast to earlier reports on complexes of neutral *primary* amines.[41] Dethreading is indicated by an emerging set of methylene proton signals (H_d, H_e), upfield shifted by $\Delta\delta \approx 0.8$ ppm upon deprotonation and dethreading. The pseudo[2]rotaxanes **PA5@TTFC8** (2,3-dimethylbenzyl end group), **PA6@TTFC8** (2-ethylbenzyl) and **PA7@TTFC8** (2-methoxybenzyl) were also subjected to deprotonation. Again, dethreading *via* deprotonation occurred immediately (see ESI Fig. S42 and Table S1‡).

The pseudorotaxane **PA11@TTFC8** can also successfully be oxidized with excess $NOSbF_6$ in dry CD_2Cl_2 under argon atmosphere. Two subsequent one-electron-oxidation steps lead to the TTF dication **PA11@TTFC8**$^{2+}$ easily recognizable from its instantaneously appearing deep blue colour. The oxidized macrocycle unthreads with a $t_{1/2}$ of 11 h (Fig. 5b, ESI section 2 Fig. S42‡). As the dication is again diamagnetic, unthreading can also be followed by integrating of a new set of methylene proton signals (H_d, H_e), upfield shifted by $\Delta\delta \approx 0.3$ and 0.6 ppm. This is confirmed by monitoring the dethreading of pseudo[2]rotaxanes **PA5@TTFC8**, **PA6@TTFC8** and **PA7@TTFC8** after oxidation. Complete dethreading occurred only for **PA7@TTFC8** and required a substantially longer time ($t_{1/2}$ = 22 h, see ESI section 2 Fig. S36‡).

These experiments clearly reveal that the dethreading rate does not only depend on the steric bulk of the axles' terminal groups, but also change significantly with the nature of the stimulus applied. Earlier, we reported attractive forces to still occur even between the doubly oxidized **TTFC8** and secondary ammonium axles.[29] Assuming that the ring circumference and conformational flexibility of **TTFC8** is not significantly altered upon oxidation[42] and taking into account that the oxidation itself occurs almost instantaneously, we therefore hypothesize that these residual interactions are the cause for the slower dethreading after oxidation. Fig. 5a qualitatively visualizes this in the framework of the energy landscapes after oxidation and after deprotonation: The oxidized pseudorotaxane resides in a somewhat lower local minimum on its potential energy surface as compared to the deprotonated pseudorotaxane.

Synthesis of 'speed bump' rotaxanes

Axle **6** (Fig. 6) features the bulky 1-naphthalene moiety and can easily be equipped with a stopper. After stirring **6** with **TTFC8** for three days at 40 °C (for **R1**, Fig. 6) or **S4** (axle of rotaxane **R2**) with **TTFC8** for 10 minutes at room temperature (for **R2**), nitrile-oxide stopper **St1**[43] was added and the mixtures were stirred at 35 °C overnight. Two rotaxanes (**R1** and **R2**) were isolated only differing by the size of the connecting blue 'speed bump'.

In the ^{1}H NMR spectra, successful rotaxane formation is evidenced by a downfield shift ($\Delta\delta$ = +0.5 ppm) of the methylene protons next to the ammonium, as well as the strong downfield shift ($\Delta\delta$ = +4.0 ppm) of the former alkyne proton that is incorporated in the newly formed isoxazole (H_p for **R1** and H_j for **R2**). Additionally, the methylene protons next to the

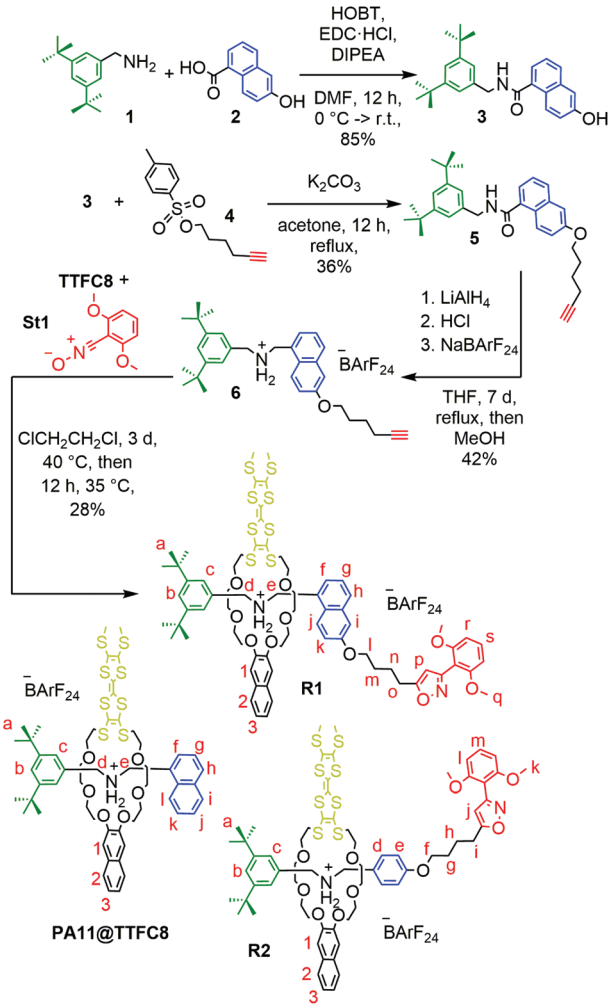

Fig. 6 Synthesis of rotaxane **R1**. Rotaxane **R2** and pseudo[2]rotaxane **PA11@TTFC8** are shown for comparison. For details of the synthesis of **R2**, see ESI, Scheme S3.‡

axle ether oxygen atom (H_l for **R1** and H_f for **R2**) shows an upfield shift ($\Delta\delta$ = 1.0 ppm) due to the close proximity to the naphthalene and/or TTF moiety of **TTFC8** (see ESI Fig. S19 and S26‡). The interlocked structure was further supported by tandem mass spectrometry. Collision-induced dissociation of mass-selected rotaxane parent ions occurred only at high collision energies. As the intact axle is not observed among the fragments, it is clear that dissociation of the two components is only possible after covalent bond cleavage within the axle, which excludes a non-threaded complex. Also, the collision energies required for dissociation as well as the observed fragment ions are comparable to other similar rotaxanes.[29]

Deprotonation of the rotaxanes

Deprotonation of **R1** with polystyrene-immobilized P2 base yields a neutral amine (Fig. 7d) which is indicated by a strong highfield shift of methylene protons $H_{d,e}$ ($\Delta\delta$ = 1 ppm solid line). The positions of these signals are similar to those of the deprotonated free axle (Fig. 7e). Other significant shifts

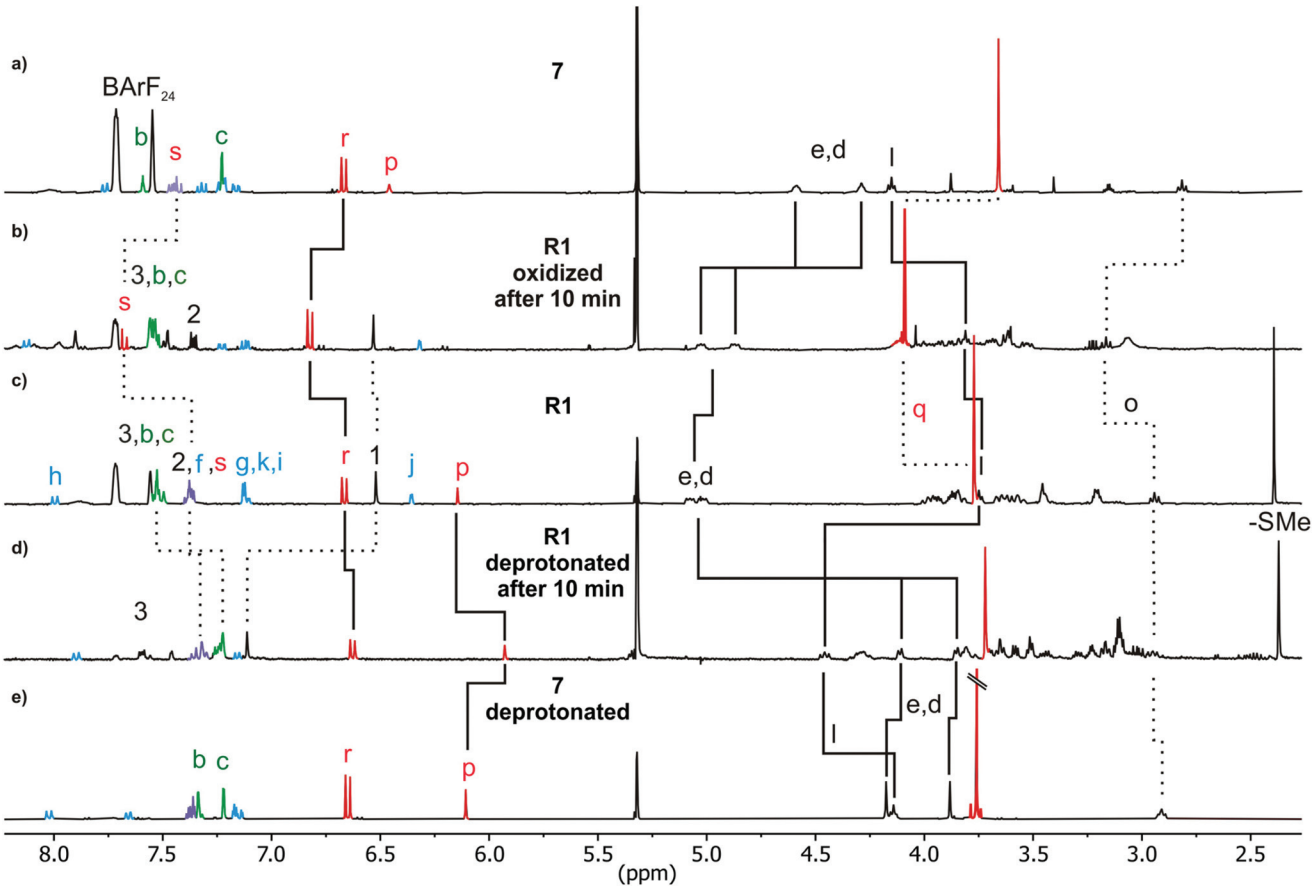

Fig. 7 ^{1}H NMR spectra (400 MHz, 298 K, CD_2Cl_2) of (a) stoppered axle **7** (b) **R1** 10 min after two-electron-oxidation (c) **R1** (d) **R1** 10 minutes after deprotonation and (e) deprotonated **7** with selected shifts highlighted.

include the isoxazole proton H_p ($\Delta\delta$ = −0.5 ppm), and alkyl chain methylene protons H_l ($\Delta\delta$ = +0.7 ppm solid line). Together with the downfield shift of H_l, this clearly indicates a deprotonation-induced shuttling away from the amine and towards the alkyl chain. No such shift of H_l is observed when free axle **7** (**6+St1**) is deprotonated (Fig. 7a/e). Rotaxane **R2** behaves similarly (Fig. S43 bottom‡). Variable temperature ^{1}H NMR experiments (see ESI, Fig. S51 and S52‡) performed with deprotonated **R1** and **R2** to test whether the two positional isomers of the wheel would be distinguishable unfortunately remained inconclusive.[24,44–50] Nevertheless, the NMR data is in agreement with a shift of the wheel across the 'speed bump' in the axle centre upon deprotonation.

Oxidation of the rotaxanes

The ^{1}H NMR spectrum of **R1** recorded 10 minutes after oxidation with $NOSbF_6$ to $\mathbf{R1}^{2+}$ is shown in Fig. 7b and did not change over the following 48 hours. The methylene protons $H_{d,e}$ next to the ammonium ion undergo only a small upfield shift ($\Delta\delta$ = −0.1 ppm). Also, proton H_l is shifted only by a small amount. As the small shifts can easily be rationalized by the additional charge induced through oxidation, these findings indicate that the wheel still occupies the ammonium station. However, protons H_r and H_s of the dimethoxyphenyl stopper at the opposite end of the axle shift downfield to some extent ($\Delta\delta$ = 0.2 to 0.25 ppm). Although this observation may at first glance seem inconsistent with the interpretation that the wheel remains on the ammonium side of the axle, these shift differences can be easily explained by invoking p-donor–p-acceptor complex formation between the strongly electron-deficient TTF^{2+} dication and the rather electron-rich dimethoxyphenyl stopper. The ^{1}H NMR spectrum of the oxidized rotaxane thus indicates that the macrocycle still encircles the ammonium ion, while refolding of the more remote axle half occurs.

More evidence can be obtained from cyclovoltammetric (CV) and differential pulse voltammetric (DPV) experiments with which the half-wave potentials of the two reversible TTF redox waves can be obtained. These potentials characteristically shift depending on the interactions between axle and wheel, as shown earlier for **TTFC8**-containing rotaxanes.[29,51,52] The correlation diagram in Fig. 8a contains the peak potentials obtained by DPV measurements in CH_2Cl_2 with n-Bu_4NBArF_{24} as the supporting electrolyte. Compared to the free wheel, the redox potentials $E^1_{1/2}(TTF^{0/+})$ and $E^2_{1/2}(TTF^{+/2+})$ are anodically shifted for all species bound to an axle. **PA12@TTFC8** is a diagnostic control compound, as two sets of TTF redox processes corresponding to the threaded ($E^1_{1/2}$, $E^2_{1/2}$) and unthreaded wheel ($E^1_{1/2}$, $E'_{1/2}$) are observed (see ESI Fig. S55‡). The low

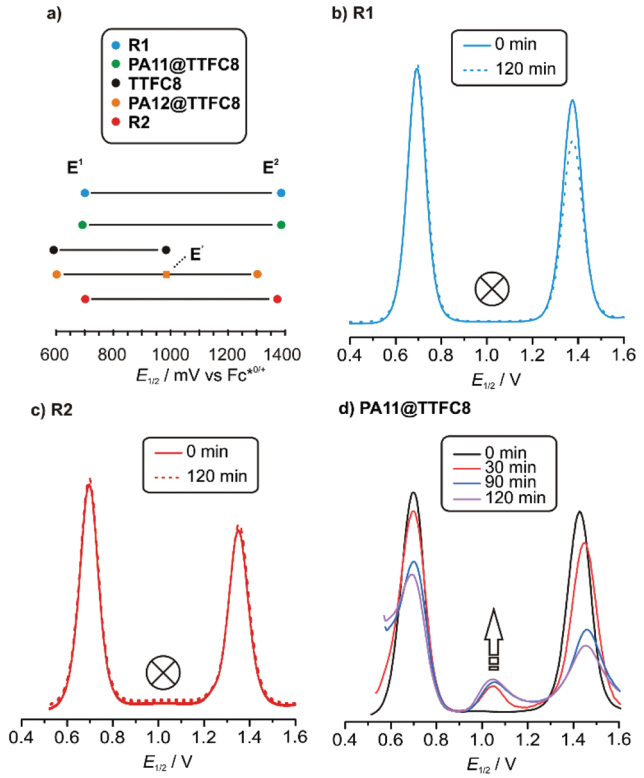

Fig. 8 Electrochemical data: (a) Correlation diagram of DPV peak potentials of all relevant (pseudo)rotaxane species, DPVs before and after electrolysis of (b) **R1**, (c) **R2**, (d) **PA11@TTFC8** (CH_2Cl_2, with *n*-Bu_4NBArF_{24} as the electrolyte (0.1 M), 298 K, 1 mM analyte, 25 mV modulation amplitude, 50 ms modulation time, 5 mV step potential, 0.5 s interval time).

steric bulk of the phenyl group allows fast interconversion between threaded and unthreaded on the CV timescale (in the DPV only one peak for $TTF^{0/+}$ redox couple is visible). In contrast, the isolated pseudorotaxane **PA11@TTFC8** only shows one redox couple for $TTF^{0/+}$ and $TTF^{+/2+}$ due to the sterically hindered unthreading. The mechanically interlocked structures **R1** and **R2** show no third feature ($E'_{1/2}$), meaning that the voltammograms indicate no significant wheel shuttling away from the ammonium station on the timescale of the experiment. Bulk electrolysis (Fig. 8b–d) of the (pseudo)rotaxanes for 2 h did not show a change in the DPV for **R1** and **R2**. However, for **PA11@TTFC8** signal broadening and lowered amperage in the course of electrolysis was observed. Bulk electrolysis gave rise to a new signal, which corresponds to the second oxidation of unbound **TTFC8**. The bulk electrolysis experiments suggest, that electrochemically–induced migration over the naphthalene moiety does take place for pseudorotaxane **PA11@TTFC8**. On the contrary, no such behavior was observed for the rotaxanes **R1** and **R2**. These results clearly support the ^{1}H NMR data, that no oxidation-induced shuttling occurs in the mechanically interlocked species.

Consequently, the behaviour of the rotaxanes parallels that of the pseudorotaxanes in that the two different stimuli cause significant differences in dethreading/shuttling rates despite of the steric barrier remaining unchanged. Also, the reason – a binding interaction of the crown ether wheel to the ammonium ion that is stronger than the effects of charge repulsion – is likely the same. Nevertheless, there are also differences: While the pseudorotaxane finally dethreads over 48 hours, no change is observed on a similar time scale for the rotaxane. This is an effect of the mechanical bond. While dethreading of the pseudorotaxane is entropically favoured by an increase in particle number, such wheel shuttling in the rotaxanes does not benefit from such entropic benefit.

Conclusions

A set of $BArF_{24}^-$ salts of *sec*-ammonium ions bearing different bulky end groups have been investigated with respect to their ability to form crown ether/ammonium pseudorotaxanes. The small differences in bond lengths between the two crown ethers **DB24C8** and **TTFC8** change the threading barrier significantly and threading occurs significantly faster for **TTFC8**. Three groups of quickly threading, kinetically hindered slowly threading, and non-threading axles can be distinguished. For the slowly and non-threading axle/wheel pairs, the formation of face-to-face crown ether/ammonium complexes occurs, which has been exemplarily studied in more detail for **PA11** by ^{1}H NMR, tandem MS and ITC experiments. To our knowledge this is the first time that an equilibrium of a threaded and non-threaded complex was quantitatively studied for the same axle macrocycle combination.

Deslipping of **TTFC8** from different axles could be achieved by deprotonation of the axle or by chemical oxidation of the macrocycle. Upon deprotonation, the pseudorotaxanes dissociate quickly. Chemical oxidation to the TTF dication lead to much slower dethreading. The difference in dethreading rates for the two stimuli can be explained by residual attractive interaction of the oxidized $\mathbf{TTFC8}^{2+}$ and the axle. It is quite remarkable that two different stimuli lead to so clearly different dethreading rates, even though the steric barrier remains unchanged. Clearly, an interplay between the steric barrier and the changes in the interactions between wheel and its binding stations is observed here which complicates the analysis of such steric 'speed bumps' in molecular interlocked switches and machines.

The shuttling of the wheel in the rotaxanes on one hand behaves similarly in that the two stimuli cause different effects on the shuttling. But the behaviour is not fully analogous. The comparison of rotaxanes and pseudorotaxanes clearly reveals a significant and non-negligible influence of the mechanical bond. At the end, the shuttling is affected by changing interactions between the wheel and the available binding stations as well as steric barriers on its way along the axle and the particular effects of the mechanical bond.

Conflicts of interest

There are no conflicts of interest to declare.

Acknowledgements

Gefördert durch die Deutsche Forschungsgemeinschaft (DFG) – Projektnummer 387284271 – SFB 1349 – und Projektnummer 434455294 (funded by the Deutsche Forschungsgemeinschaft – project-ID 387284271 – SFB 1349 and project-ID 434455294). A.V. kindly acknowledges the Academy of Finland (grant no. 314343) for financial support. We also thank Jennifer Anders for help with the synthesis.

Notes and references

1 J. D. Harris, M. J. Moran and I. Aprahamian, New molecular switch architectures, *Proc. Natl. Acad. Sci. U. S. A.*, 2018, **115**, 9414–9422.
2 J. D. Badjic, V. Balzani, A. Credi, S. Silvi and J. F. Stoddart, A molecular elevator, *Science*, 2004, **303**, 1845–1849.
3 D. Cao, Z. Liu, P. Verwilst, S. Koo, P. Jangjili, J. S. Kim and W. Lin, Coumarin-Based Small-Molecule Fluorescent Chemosensors, *Chem. Rev.*, 2019, **119**, 10403–10519.
4 D. Bleger and S. Hecht, Visible-Light-Activated Molecular Switches, *Angew. Chem., Int. Ed.*, 2015, **54**, 11338–11349.
5 D. Dattler, G. Fuks, J. Heiser, E. Moulin, A. Perrot, X. Yao and N. Giuseppone, Design of Collective Motions from Synthetic Molecular Switches, Rotors, and Motors, *Chem. Rev.*, 2020, **120**, 310–433.
6 A. Coskun, J. M. Spruell, G. Barin, W. R. Dichtel, A. H. Flood, Y. Y. Botros and J. F. Stoddart, High hopes: can molecular electronics realise its potential?, *Chem. Soc. Rev.*, 2012, **41**, 4827–4859.
7 S. Erbas-Cakmak, D. A. Leigh, C. T. McTernan and A. L. Nussbaumer, Artificial Molecular Machines, *Chem. Rev.*, 2015, **115**, 10081–10206.
8 E. R. Kay, D. A. Leigh and F. Zerbetto, Synthetic molecular motors and mechanical machines, *Angew. Chem., Int. Ed.*, 2007, **46**, 72–191.
9 T. Felder and C. A. Schalley, Secondary isotope effects on the deslipping reaction of rotaxanes: high-precision measurement of steric size, *Angew. Chem., Int. Ed.*, 2003, **42**, 2258–2260.
10 E. A. Neal and S. M. Goldup, Chemical consequences of mechanical bonding in catenanes and rotaxanes: isomerism, modification, catalysis and molecular machines for synthesis, *Chem. Commun.*, 2014, **50**, 5128–5142.
11 M. Baroncini, S. Silvi and A. Credi, Photo- and Redox-Driven Artificial Molecular Motors, *Chem. Rev.*, 2020, **120**, 200–268.
12 Z. Liu, S. K. M. Nalluri and J. F. Stoddart, Surveying macrocyclic chemistry: from flexible crown ethers to rigid cyclophanes, *Chem. Soc. Rev.*, 2017, **46**, 2459–2478.
13 A. Carrasco-Ruiz and J. Tiburcio, Electrostatic kinetic barriers in the threading/dethreading motion of a rotaxane-like complex, *Org. Lett.*, 2015, **17**, 1858–1861.
14 P. R. Ashton, P. J. Campbell, P. T. Glink, D. Philp, N. Spencer, J. F. Stoddart, E. J. T. Chrystal, S. Menzer, D. J. Williams and P. A. Tasker, Dialkylammonium Ion/Crown Ether Complexes: The Forerunners of a New Family of Interlocked Molecules, *Angew. Chem., Int. Ed. Engl.*, 1995, **34**, 1865–1869.
15 R. M. Izatt, J. D. Lamb, N. E. Izatt, B. E. Rossiter, J. J. Christensen and B. L. Haymore, A calorimetric titration study of the reaction of several organic ammonium cations with 18-crown-6 in methanol, *J. Am. Chem. Soc.*, 1979, **101**, 6273–6276.
16 P. R. Ashton, I. Baxter, M. C. T. Fyfe, F. M. Raymo, N. Spencer, J. F. Stoddart, A. J. P. White and D. J. Williams, Rotaxane or Pseudorotaxane? That Is the Question!†, *J. Am. Chem. Soc.*, 1998, **120**, 2297–2307.
17 C. J. Bruns and J. F. Stoddart, *The Nature of the Mechanical Bond: From Molecules to Machines*, John Wiley & Sons, Inc., 2016.
18 T. Clifford, A. Abushamleh and D. H. Busch, Factors affecting the threading of axle molecules through macrocycles: binding constants for semirotaxane formation, *Proc. Natl. Acad. Sci. U. S. A.*, 2002, **99**, 4830–4836.
19 J. Groppi, L. Casimiro, M. Canton, S. Corra, M. Jafari-Nasab, G. Tabacchi, L. Cavallo, M. Baroncini, S. Silvi, E. Fois and A. Credi, Precision Molecular Threading/Dethreading, *Angew. Chem., Int. Ed. Engl.*, 2020, **59**, 14825–14834.
20 P. G. Young, K. Hirose and Y. Tobe, Axle length does not affect switching dynamics in degenerate molecular shuttles with rigid spacers, *J. Am. Chem. Soc.*, 2014, **136**, 7899–7906.
21 M. Asakawa, P. R. Ashton, R. Ballardini, V. Balzani, M. Bělohradský, M. T. Gandolfi, O. Kocian, L. Prodi, F. M. Raymo, J. F. Stoddart and M. Venturi, The Slipping Approach to Self-Assembling [n]Rotaxanes†, *J. Am. Chem. Soc.*, 1997, **119**, 302–310.
22 B. Riss-Yaw, C. Clavel, P. Laurent and F. Coutrot, The relationship between the conformational degree of freedom of template-containing threads and slippage in the formation of [2]rotaxane building blocks, *Chem. Commun.*, 2017, **53**, 10874–10877.
23 Y. Yamashita, Y. Saito, S. Kikkawa, Y. Mutoh, S. Hosoya, I. Azumaya and S. Saito, Evaluation of the Steric Bulk of Substituents Utilizing the Shuttling Behavior of [2]Rotaxanes with N-Arylpyrrole Moieties, *Eur. J. Org. Chem.*, 2019, **2019**, 3412–3420.
24 G. Gholami, K. Zhu, G. Baggi, E. Schott, X. Zarate and S. J. Loeb, Influence of axle length on the rate and mechanism of shuttling in rigid H-shaped [2]rotaxanes, *Chem. Sci.*, 2017, **8**, 7718–7723.
25 A. C. Catalan and J. Tiburcio, Self-assembly of pseudorotaxane and rotaxane complexes using an electrostatic slippage approach, *Chem. Commun.*, 2016, **52**, 9526–9529.
26 C. Pezzato, C. Cheng, J. F. Stoddart and R. D. Astumian, Mastering the non-equilibrium assembly and operation of molecular machines, *Chem. Soc. Rev.*, 2017, **46**, 5491–5507.
27 G. Ragazzon, C. Schafer, P. Franchi, S. Silvi, B. Colasson, M. Lucarini and A. Credi, Remote electrochemical modu-

lation of pKa in a rotaxane by co-conformational allostery, *Proc. Natl. Acad. Sci. U. S. A.*, 2018, **115**, 9385–9390.

28 K. Nakazono and T. Takata, Neutralization of a sec-ammonium group unusually stabilized by the "rotaxane effect": synthesis, structure, and dynamic nature of a "free" sec-amine/crown ether-type rotaxane, *Chem. – Eur. J.*, 2010, **16**, 13783–13794.

29 H. V. Schröder, S. Sobottka, M. Nössler, H. Hupatz, M. Gaedke, B. Sarkar and C. A. Schalley, Impact of mechanical bonding on the redox-switching of tetrathiafulvalene in crown ether-ammonium [2]rotaxanes, *Chem. Sci.*, 2017, **8**, 6300–6306.

30 H. Hupatz, M. Gaedke, H. V. Schröder, J. Beerhues, A. Valkonen, F. Klautzsch, S. Müller, F. Witte, K. Rissanen, B. Sarkar and C. A. Schalley, Thermodynamic and electrochemical study of tailor-made crown ethers for redox-switchable (pseudo)rotaxanes, *Beilstein J. Org. Chem.*, 2020, **16**, 2576–2588.

31 A. Crochet, E. Kottelat, A. Fleury, M. Neuburger and K. M. Fromm, Polymorph of Dibenzo-24-Crown-8 and its Mercury Complex, *Z. Anorg. Allg. Chem.*, 2011, **637**, 672–675.

32 H. Nagai, Y. Suzaki and K. Osakada, Thiacrown Ethers with Oxygen and Sulfur for Coordination: Formation of the Pd and Pt Complexes and Pseudorotaxane with Dialkylammonium, *Eur. J. Inorg. Chem.*, 2014, **2014**, 4376–4384.

33 F. Le Derf, M. Mazari, N. Mercier, E. Levillain, P. Richomme, J. Becher, J. Garin, J. Orduna, A. Gorgues and M. Salle, Electroregulated Metal-Binding with a Crown Ether Tetrathiafulvalene Derivative: Toward Electrochemically Addressed Metal Cation Sponges, *Inorg. Chem.*, 1999, **38**, 6096–6100.

34 H. Nagai, Y. Suzaki and K. Osakada, Chemical Modification of a [2]Rotaxane Composed of Dithiacrown Ether and Dialkylammonium with Organic and Inorganic Compounds, *Chem. Lett.*, 2016, **45**, 834–836.

35 A. R. Williams, B. H. Northrop, K. N. Houk, J. F. Stoddart and D. J. Williams, The influence of constitutional isomerism and change on molecular recognition processes, *Chem. – Eur. J.*, 2004, **10**, 5406–5421.

36 S. J. Cantrill, D. A. Fulton, A. M. Heiss, A. R. Pease, J. F. Stoddart, A. J. P. White and D. J. Williams, The Influence of Macrocyclic Polyether Constitution upon Ammonium Ion/Crown Ether Recognition Processes, *Chem. – Eur. J.*, 2000, **6**, 2274–2287.

37 T. Takata, Stimuli-Responsive Molecular and Macromolecular Systems Controlled by Rotaxane Molecular Switches, *Bull. Chem. Soc. Jpn.*, 2019, **92**, 409–426.

38 S. Miyagawa, M. Kimura, S. Kagami, T. Kawasaki and Y. Tokunaga, Utilization of a Crown Ether/Amine-Type Rotaxane as a Probe for the Versatile Detection of Anions and Acids by Thin-Layer Chromatography, *Chem. – Asian J.*, 2020, **15**, 3044–3049.

39 J. Nishiyama, Y. Makita and N. Kihara, Rapid and Efficient Acylative Active Transport on a Rotaxane, *Asian J. Org. Chem.*, 2015, **4**, 1056–1064.

40 H. Sato, D. Aoki and T. Takata, Synthesis and Star/Linear Topology Transformation of a Mechanically Linked ABC Terpolymer, *ACS Macro Lett.*, 2016, **5**, 699–703.

41 S. D. P. Fielden, D. A. Leigh, C. T. McTernan, B. Perez-Saavedra and I. J. Vitorica-Yrezabal, Spontaneous Assembly of Rotaxanes from a Primary Amine, Crown Ether and Electrophile, *J. Am. Chem. Soc.*, 2018, **140**, 6049–6052.

42 H. V. Schröder, F. Witte, M. Gaedke, S. Sobottka, L. Suntrup, H. Hupatz, A. Valkonen, B. Paulus, K. Rissanen, B. Sarkar and C. A. Schalley, An aryl-fused redox-active tetrathiafulvalene with enhanced mixed-valence and radical-cation dimer stabilities, *Org. Biomol. Chem.*, 2018, **16**, 2741–2747.

43 T. Matsumura, F. Ishiwari, Y. Koyama and T. Takata, C-C bond-forming click synthesis of rotaxanes exploiting nitrile N-oxide, *Org. Lett.*, 2010, **12**, 3828–3831.

44 V. N. Vukotic, K. Zhu, G. Baggi and S. J. Loeb, Optical Distinction between "Slow" and "Fast" Translational Motion in Degenerate Molecular Shuttles, *Angew. Chem., Int. Ed.*, 2017, **56**, 6136–6141.

45 K. Hirose, Molecular brake systems controlled by light and heat, *J. Inclusion Phenom. Macrocyclic Chem.*, 2010, **68**, 1–24.

46 J. Dale and P. O. Kristiansen, Cyclic oligo-ethers related to ethylene oxide, *J. Chem. Soc., Chem. Commun.*, 1971, **13**, 670.

47 C. I. Ratcliffe, J. A. Ripmeester, G. W. Buchanan and J. K. Denike, A molecular merry-go-round: motion of the large macrocyclic molecule 18-crown-6 in its solid complexes studied by deuterium NMR, *J. Am. Chem. Soc.*, 1992, **114**, 3294–3299.

48 V. N. Vukotic, K. J. Harris, K. Zhu, R. W. Schurko and S. J. Loeb, Metal-organic frameworks with dynamic interlocked components, *Nat. Chem.*, 2012, **4**, 456–460.

49 K. Zhu, V. N. Vukotic, C. A. O'Keefe, R. W. Schurko and S. J. Loeb, Metal-organic frameworks with mechanically interlocked pillars: controlling ring dynamics in the solid-state via a reversible phase change, *J. Am. Chem. Soc.*, 2014, **136**, 7403–7409.

50 N. D. Suhan, L. Allen, M. T. Gharib, E. Viljoen, S. J. Vella and S. J. Loeb, Colour coding the co-conformations of a [2] rotaxane flip-switch, *Chem. Commun.*, 2011, **47**, 5991–5993.

51 M. Gaedke, F. Witte, J. Anhäuser, H. Hupatz, H. V. Schröder, A. Valkonen, K. Rissanen, A. Lützen, B. Paulus and C. A. Schalley, Chiroptical inversion of a planar chiral redox-switchable rotaxane, *Chem. Sci.*, 2019, **10**, 10003–10009.

52 H. V. Schröder, F. Stein, J. M. Wollschläger, S. Sobottka, M. Gaedke, B. Sarkar and C. A. Schalley, Accordion-Like Motion in Electrochemically Switchable Crown Ether/Ammonium Oligorotaxanes, *Angew. Chem., Int. Ed.*, 2019, **58**, 3496–3500.